



## Heterogeneous photocatalytic degradation of reactive dyes in aqueous TiO<sub>2</sub> suspensions: Decolorization kinetics

Raphael B.M. Bergamini<sup>a</sup>, Eduardo B. Azevedo<sup>b</sup>, Lucia R. Raddi de Araújo<sup>a,\*</sup>

<sup>a</sup> Physical Chemistry Department, Universidade do Estado do Rio de Janeiro, Rua São Francisco Xavier, 524 Maracanã, Rio de Janeiro/RJ, CEP 20550–900, Brazil

<sup>b</sup> Molecular Chemistry and Physics Department, Instituto de Química de São Carlos (IQSC), Universidade de São Paulo (USP), Av. Trabalhador São-Carlense, 400 – Centro, São Carlos/SP, CEP 13560–970, Brazil

### ARTICLE INFO

#### Article history:

Received 17 July 2008

Received in revised form 7 October 2008

Accepted 17 October 2008

#### Keywords:

Photocatalysis

TiO<sub>2</sub>

Dyes

Textile industry

### ABSTRACT

This work assesses the photocatalytic (TiO<sub>2</sub>/UV) degradation of a simulated reactive dye bath (Black 5, Red 239, Yellow 17, and auxiliary chemicals). Color removal was monitored by spectrophotometry. Mineralization was determined by DOC analyses. Photocatalytic, photolytic, and adsorption experiments were performed, showing that adsorption was negligible. After 30 min of irradiation, it was achieved 97% and 40% of color removal with photocatalysis and photolysis, respectively. No mineralization occurred within 30 min. A kinetic model composed of two first-order in-series reactions was used. The first photocatalytic decolorization rate constant was  $k_1 = 2.6 \text{ min}^{-1}$  and the second  $k_2 = 0.011 \text{ min}^{-1}$ . The fast decolorization of Reactive Black 5 dye is an indication that the number of azo and vinylsulfone groups in the dye molecule may be a determining factor for the increased photolytic and photocatalytic color removal and degradation rates.

© 2008 Elsevier B.V. All rights reserved.

### 1. Introduction

Many industries contribute to contaminate the environment, especially water resources. The main environmental impacts caused by the textile industry involve its high water consumption (for instance, 80–100 L kg<sup>-1</sup> of cotton [1]) and the low fixation degree of raw materials, such as starching agents, detergents, dyes and others. These two factors lead to the generation of large volumes of wastewaters containing high organic loads and strong color [2].

Traditional methods of treatment have the major disadvantage of being phase-transfer methods, which require subsequent treatment or disposal. On the other hand, biological treatments (which are destructive) take a long time for the effluent to reach the required standards and produce a large quantity of sludge, which normally cannot be reused [3].

Advanced oxidative processes (AOPs) have been attracting considerable interest because they are more effective and sustainable in the long term. They are technologies that generally use a strong oxidizing agent (O<sub>3</sub>, H<sub>2</sub>O<sub>2</sub>) and/or catalyst (Fe, TiO<sub>2</sub>) in the presence or absence of a source of irradiation, generating highly reactive hydroxyl radicals (HO<sup>•</sup>). Those radicals are able to mineralize refrac-

tory organic substances that are present in industrial effluents [4]. Among the various AOPs, heterogeneous photocatalysis has been researched exhaustively in recent decades, particularly from the standpoint of degradation of effluents produced by the textile industry [5–8].

The effluents from the dyeing process of textile fibers and fabric can modify the ecosystem, reducing the transparency of water and the sunlight penetration, and thereby altering the photosynthetic activity and the solubility of gases. Up to 40% of the loads of these effluents may consist of dyes used in dyeing processes [9].

According to the method of fixation to the textile fiber, dyes are classified into various types, such as acid, basic, direct, dispersed, reactive, and others. Reactive dyes are a class of dyes whose use in the textile industry has grown steadily due to their reactivity with fibers and their color stability. For this reason they are also one of the dyes most widely reported in the literature [5,10–15].

The production process of reactive dyes, which was patented in 1956, consists of introducing an electrophilic (reactive) group into the dye. This reactive group binds covalently to the molecules of the fabric fibers, and only since the introduction of this technique cotton has been successfully dyed with strong colors. Reactive dyes are highly soluble in water and have a high degree of reactivity with cellulose fibers (cotton, linen, viscose) and with the amine, hydroxyl or thiol groups of protein fibers (wool, silk). Presently, one of the most common reactive groups is the vinylsulfone one (–SO<sub>2</sub>CH=CH<sub>2</sub>).

\* Corresponding author. Tel.: +55 21 25877848; fax: +55 21 25877172.  
E-mail address: [luraddi@uerj.br](mailto:luraddi@uerj.br) (L.R.R.d. Araújo).

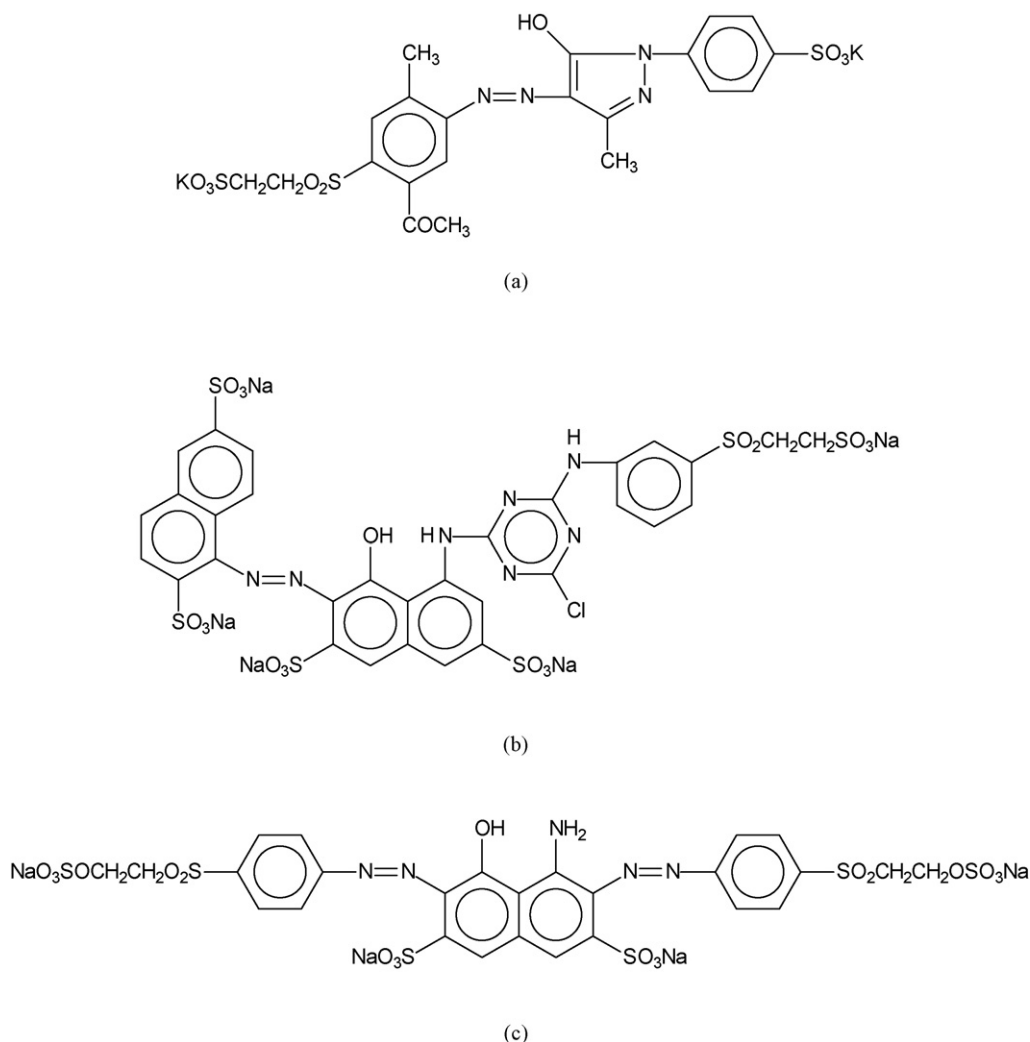


Fig. 1. Chemical structures of the reactive dyes: (a) Yellow 17, (b) Red 239, and (c) Black 5.

The objective of this study is to assess the feasibility of heterogeneous photocatalysis (using TiO<sub>2</sub> as the photocatalyst and UV light) in the decolorization of a simulated dye bath containing vinylsulfone-type reactive azo dyes.

## 2. Experimental and methods

### 2.1. Dyes

The studied dyes, presented in Fig. 1, were chosen due to their widespread usage in the textile industry. They are C.I. Reactive Black 5, C.I. Reactive Red 239, and C.I. Reactive Yellow 17. The basic difference between them is that the first one has two azo groups and two vinylsulfone groups, while the other two have only one of each.

### 2.2. Dyes bath

The degradation experiments were performed with a simulated cotton dyeing bath typical of the textile industry. In this bath, the three dyes were mixed together up to a concentration of 70 mg L<sup>-1</sup> each. Sodium chloride (50 g L<sup>-1</sup>) and sodium carbonate (5.0 g L<sup>-1</sup>) were also added. The pH of the bath was approximately 11.

### 2.3. Experimental procedure

Experiments were carried out in a 250 mL thermostated cylindrical Pyrex reactor, open to air, containing 50 mL of the bath. The photocatalyst was maintained in suspension by magnetic stirring. In all experiments, air was bubbled continuously through the suspension. The suspension was irradiated with a 250 W Phillips HPL-N medium pressure mercury vapor lamp, with the outer bulb removed, placed 12 cm above the suspension (radiant flux of 108 kJ m<sup>-2</sup> s<sup>-1</sup> at λ > 254 nm, measured with a Cole-Parmer radiometer EW-09811-54). All experiments were performed at 25 ± 1 °C. The previously determined optimum concentration of TiO<sub>2</sub> (Degussa P25, 30 nm particle size, and 50 ± 15 m<sup>2</sup> g<sup>-1</sup> BET surface area) in suspension was 4.0 g L<sup>-1</sup>. In order to remove photocatalyst particles before analyses, samples were filtered through 0.45 μm pore size cellulose acetate filters. Photolysis and adsorption control experiments were also performed. All experiments were performed in triplicate, so that the averaged values are shown.

### 2.4. Analyses

Samples were irradiated until the photocatalytic color removal reached at least approximately 90%. This criterion was followed by integrating the spectra obtained by scanning the samples from

**Table 1**  
Wavelengths of maximum absorbance and absorptivities of the dyes.

$\lambda_{\max}$ (nm)	Absorptivities ( $\text{Lmg}^{-1} \text{cm}^{-1}$ )		
	Yellow 17	Red 239	Black 5
429	0.0168	0.00446	0.00920
541	0	0.0277	0.0215
598	0	0	0.0351

400 to 700 nm (visible region) with an Agilent 8453 spectrophotometer. Dissolved organic carbon (DOC) was also measured with a Shimadzu TOC-VCPH Carbon Analyzer.

The degradation of each dye was followed by applying the Lambert–Beer equation to the measured absorbances at their respective  $\lambda_{\max}$  and the previously determined absorptivities, shown in Table 1. The system of linear equations was then solved to obtain the concentration of each dye.

### 3. Results and discussion

#### 3.1. UV–visible spectrophotometry

Adsorption control experiments showed no significant adsorption of the dyes onto the  $\text{TiO}_2$  surface. On the other hand, photolysis has proven to play an important role in the degradation of the

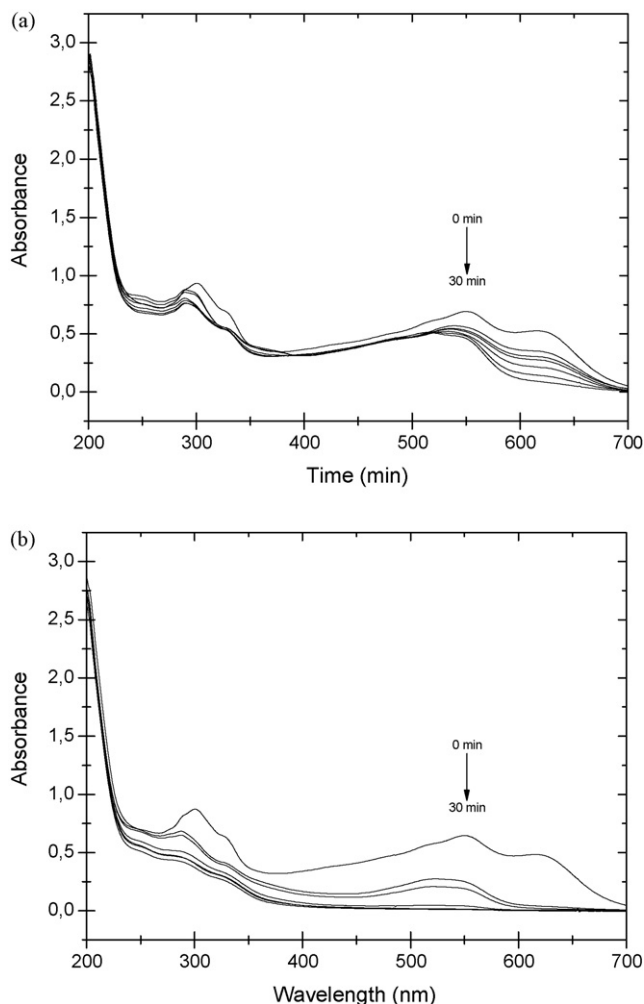


**Fig. 2.** UV–visible absorption spectra obtained at degradation times ranging from 0 to 30 min: (a) photolysis and (b) photocatalysis.

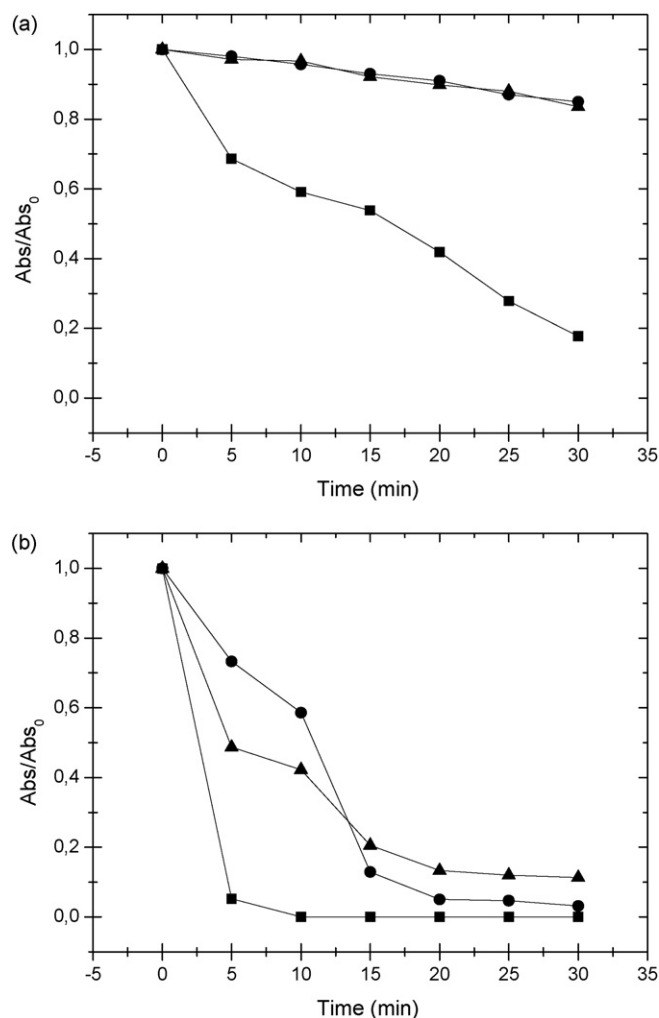


**Fig. 3.** Degradation profiles vs. time for each acid dye (■) Black 5, (●) Red 239, and (▲) Yellow 17: (a) photolysis and (b) photocatalysis.

studied dyes. Changes in absorbance spectra of irradiated-only samples are shown in Fig. 2a. It can be seen that Black 5 is efficiently photolytically degraded; the same cannot be said regarding Red 239 and Yellow 17, although some degradation is observed. Fig. 2b shows the changes with the photocatalytically system, which presents a significantly improved performance, mainly regarding Red 239 and Yellow 17. All three dyes were thoroughly degraded within 30 min of irradiation.

Fig. 3 shows the degradation profiles obtained after solving the linear system of Lambert–Beer equations. Photolysis is able to almost destroy Black 5 within 30 min of irradiation (82% of the dye was degraded), as can be seen in Fig. 3a. Completely different is the behavior of Red 239 and Yellow 17. Within the same period of irradiation, only approximately 15% of degradation was observed. By observing Fig. 3b, one can see that, during photocatalysis, the degradation rates of the dyes were dramatically improved. Black 5 was essentially degraded within 10 min of irradiation. If one compares the first 5 min of reaction, photocatalysis showed to be three times faster than photolysis. Regarding Red 239 and Yellow 17, they have shown somewhat similar patterns of degradation, which were fast in the first 20 min but remained almost the same after that. The degradation degree after 30 min was much higher, reaching around 89% and 97% for Yellow 17 and Red 239, respectively. The greater removal of Black 5 when compared to the other two dyes

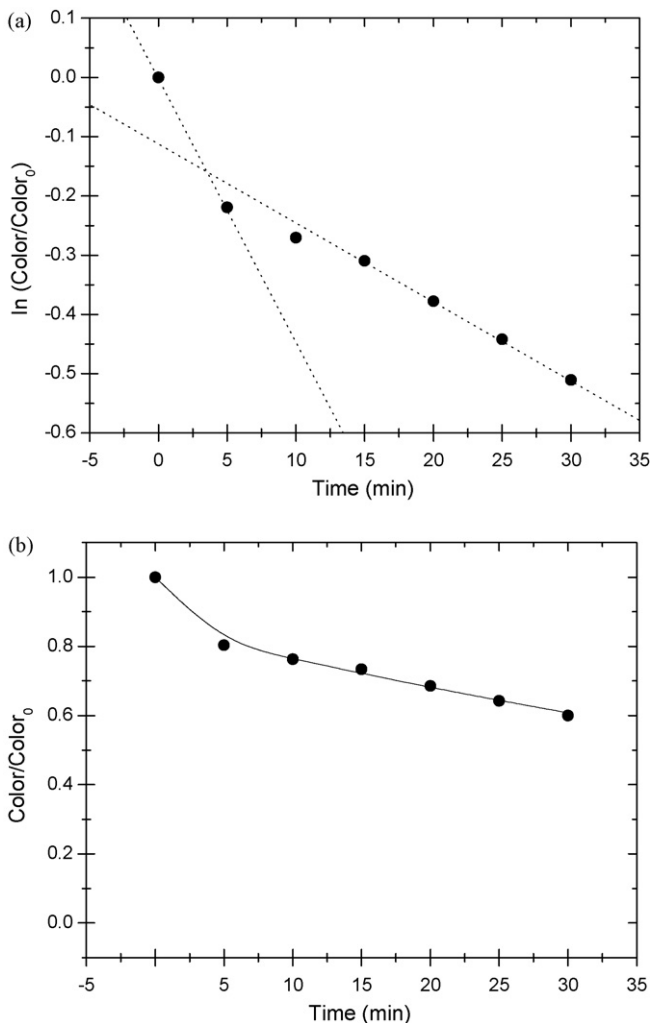


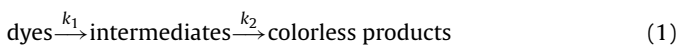
Fig. 4. Photolytic color removal kinetic modeling: (a) plot suggesting a two first-order in-series reaction model and (b) model fitted to the experimental data.

could be explained by the fact that it has two azo and two vinylsulfone groups, which are susceptible to photolytic and photocatalytic degradation [8,16].

### 3.2. Kinetic modeling and decolorization rates

The objective of this work is to assess the feasibility of heterogeneous photocatalysis for color removal of the dye bath. Therefore, the decolorization kinetics and the respective rates were investigated. Other works indicate that photocatalytic dye degradation in liquid systems can be described by first-order kinetics [17–20]. Then, it was checked if this model could be applied to the data for the photolytic color removal of the dyes bath. However, the semilog data plot, shown in Fig. 4a, does not produce a single straight line. Therefore, a simple first-order model is not suited for the entire period of irradiation.

In fact, the semilog plot of absorbance vs. time shows two regions (dashed lines), suggesting a two first-order in-series reaction model, as depicted by Eq. (1). The same approach has been used to model the photocatalytic degradation of Acid Blue 9 in solid phase [21].



Assuming that both reactions are first-order, the batch model for the concentration of the dyes,  $C_D$ , and of the intermediates,  $C_I$ , with time can be described by Eqs. (2) and (3), with the following boundary conditions:  $t = 0$ ;  $C_D = C_{D,0}$ ; and  $C_I = 0$ .

$$\frac{dC_D}{dt} = -k_1 C_D \Rightarrow C_{D,0} e^{-k_1 t} \quad (2)$$

$$\frac{dC_I}{dt} = k_1 C_D - k_2 C_I \Rightarrow C_I = \left( \frac{k_1 C_{D,0}}{k_2 - k_1} \right) (e^{-k_1 t} - e^{-k_2 t}) \quad (3)$$

Measured absorbances are the sum of contributions from the dyes and intermediates; therefore, the Lambert–Beer and Eqs. (2) and (3) were used to obtain Eq. (4), where  $a_D$  and  $a_I$  are the absorptivities of the dyes and the intermediates, respectively.

$$\text{Abs}_t = \text{Abs}_0 \left[ e^{-k_1 t} + \left( \frac{a_I}{a_D} \frac{k_1}{k_2 - k_1} \right) (e^{-k_1 t} - e^{-k_2 t}) \right] \quad (4)$$

The parameters  $k_1$ ,  $k_2$ , and the ratio  $a_I/a_D$  were first estimated by evaluating the limiting values of  $\text{Abs}_t$ . For long times, it was assumed that  $k_1$  is greater than  $k_2$  ( $e^{-k_2 t} \gg e^{-k_1 t}$ ), yielding Eq. (5). Data obtained for degradation times greater than 20 min were fit to Eq. (5) to obtain  $k_2$  and the slope ( $S$ ) of the best fitted line.

$$\frac{\text{Abs}_t}{\text{Abs}_0} = -S e^{-k_2 t}, \quad \text{where } S = \left( \frac{a_I}{a_D} \frac{k_1}{k_2 - k_1} \right) \quad (5)$$

For short times, the exponential terms in Eq. (4) were expanded to provide the first two terms in the series and rearranged to give Eq. (6). Data obtained for degradation times up to 15 min, together with  $k_2$  and  $S$  estimates, were fitted to Eq. (6), yielding an estimate of  $k_1$ .

$$k_1 = \frac{1 - S k_2 t - (\text{Abs}_t/\text{Abs}_0)}{t(1 + S)} \quad (6)$$

Finally, it was performed a non-linear curve fit to the absorbance data, using the Levenberg–Marquardt algorithm. By using Eq. (4), the obtained estimates were used as initial guesses for the kinetic parameters. The values determined for  $k_1$  and  $k_2$  were  $3.0 \pm 1.8 \text{ min}^{-1}$  and  $0.12 \pm 0.027 \text{ min}^{-1}$ , respectively, with a determination coefficient,  $R^2$ , of 0.993. As  $k_1$  is 25 times greater than  $k_2$ , the initial assumption of  $k_1 \gg k_2$  is valid. Fig. 4b shows the kinetic model fitted to the experimental data. It can be seen that the proposed model is able not only to represent the solid-phase photocatalytic degradation of an acid dye [21], but also the photolytic color removal of the simulated dye bath containing three different reactive dyes. Fig. 4b also shows that approximately 40% of the initial color was removed by the photolytic process. The same procedure was applied to the data for the photocatalytic color removal of the dyes bath.

After obtaining the initial guesses as previously described and performing the fitting procedure, the values determined for  $k_1$  and  $k_2$  were  $2.6 \pm 0.75 \text{ min}^{-1}$  and  $0.011 \pm 0.00070 \text{ min}^{-1}$ , respectively, with a determination coefficient,  $R^2$ , of 0.998. As  $k_1$  is approximately 240 times greater than  $k_2$ , again the initial assumption of  $k_1 \gg k_2$  is valid. Fig. 5b shows the kinetic model fitted to the experimental data. It can be seen that the proposed model is also able to represent the photocatalytic color removal of the simulated dye bath. Fig. 5b also shows that approximately 97% of the initial color was removed by the photocatalytic process. By comparing the photolytic and photocatalytic process ( $k_1$  and  $k_2$ ), one can see that, statistically, within a 95% of confidence limit, there is no difference in the values of  $k_1$ . This is probably due to the Black 5 behavior of being significantly degraded by both processes. For both processes, the initial reaction of turning the dyes into intermediates is much faster than the one that turn the latter into colorless products.

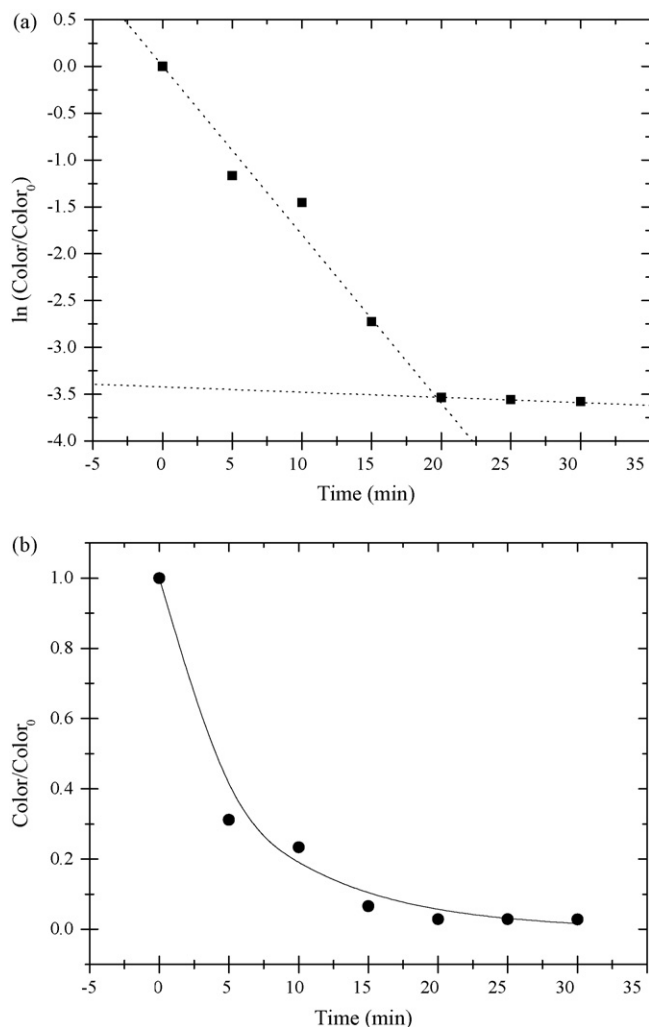


**Fig. 5.** Photocatalytic color removal kinetic modeling: (a) plot suggesting a two first-order in-series reaction model and (b) model fitted to the experimental data.

### 3.3. Dissolved organic carbon and mineralization degree

In order to obtain a suitable concentration profile vs. time for both processes, lumps were defined as follows: lump 1, dyes; lump 2, intermediates; and lump 3,  $\text{CO}_2$ . Dyes concentrations,  $C_D$ , in  $\text{mg}_{\text{Dyes}} \text{L}^{-1}$ , determined by spectrophotometry, were converted into  $\text{mg}_{\text{DOC}} \text{L}^{-1}$  by Eq. (7), where  $m(C)$  stands for the weight of carbon in the dye molecule and  $m(\text{Dye})$  for the dye molar weight.

$$\text{mg}_{\text{Dyes}} \text{L}^{-1} = \frac{m(C)}{m(\text{Dye})} \text{mg}_{\text{DOC}} \text{L}^{-1} \quad (7)$$

The intermediates concentrations,  $C_I$ , were determined by Eq. (8), where  $C_C$  stands for  $\text{CO}_2$  concentrations.

$$C_I = \text{DOC}_0 - (C_D + C_C) \quad (8)$$

Finally,  $C_C$  is calculated by Eq. (9), where  $\text{DOC}_0$  is the initial organic carbon concentration and  $\text{DOC}_t$  are the ones determined during degradation.

$$C_C = \text{DOC}_0 - \text{DOC}_t \quad (9)$$

Fig. 6 shows the obtained profiles using the above methodology. In Fig. 6a, related to photolysis, it becomes clear that no mineralization occurred. All of the dyes were converted to their respective intermediates, which build up in the system. Fig. 6b presents a simi-

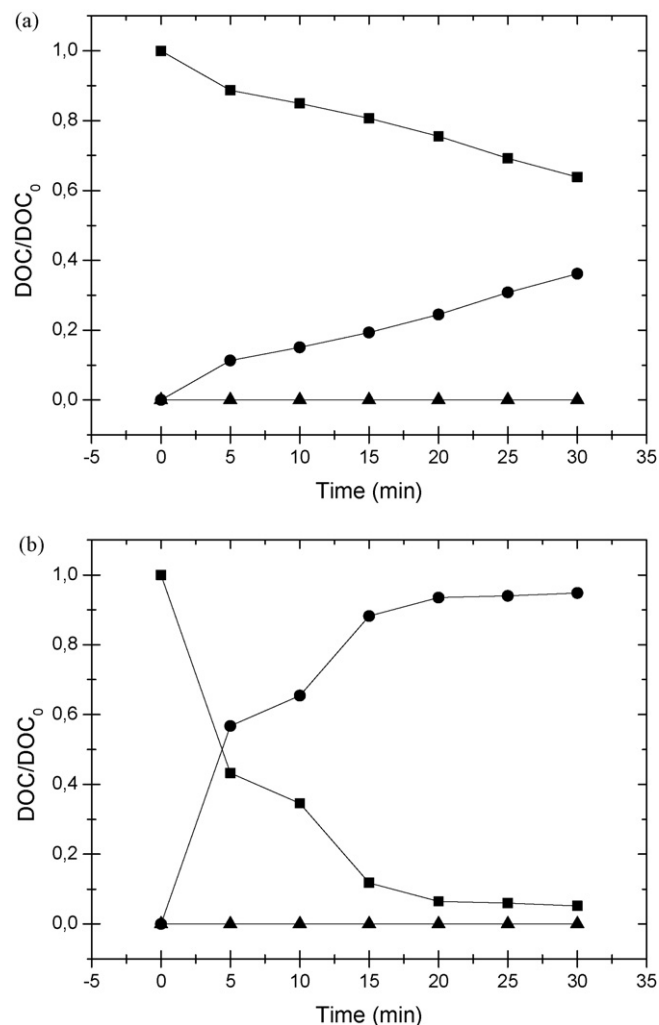


**Fig. 6.** Lumps concentration profiles (■) dyes, (●) intermediates, and (▲)  $\text{CO}_2$ : (a) photolysis and (b) photocatalysis.

lar behavior during the photocatalytic process, the difference being the concentration of intermediates, which is significantly higher. Therefore, it can be postulated that the intermediates produced by photocatalysis are not amenable to be mineralized during periods of time (up to 30 min) which are enough for color removal. In fact, other works in the literature report the dyes can be effectively degraded by photocatalysis, but several hours of irradiation are needed for that [5,22–25].

## 4. Conclusions

Regarding photolysis, C.I. Reactive Red 239 and C.I. Reactive Yellow 17 showed a comparable rate which was far less significant than C.I. Reactive Black 5. However, photocatalysis was much more efficient for the degradation of all three dyes.

The proposed model of two first-order in-series reactions described nicely the color removal process. It was observed that the dyes degradation rate into colored intermediates is more than one order of magnitude greater than the one of the intermediates into colorless products. No mineralization was observed during color removal.

It may be postulated that the dyes color removal and degradation rates are proportional to the number of azo and vinylsulfone groups present in their molecules.

In summary, this work demonstrates that photocatalysis is a very effective technology for degrading reactive dyes with azo and vinylsulfone groups. Moreover, this technology can be utilized directly in dye baths before they are mixed with other textile effluents, which makes their treatment difficult and costly due to dilution.

### Acknowledgements

The authors want to thank Degussa for kindly supplying TiO<sub>2</sub> and CAPES (Brazil) for financial support.

### References

- [1] D.E. Kritikos, N.P. Xekoukoulotakis, E. Psillakis, D. Mantzavinos, Photocatalytic degradation of Reactive Black 5 in aqueous solutions: effect of operatin conditions and coupling with ultrasound irradiation, *Water Res.* 41 (10) (2007) 2236–2246.
- [2] R.R. Souza, I.T.L. Bresolin, T.L. Bioni, M.L. Gimenes, B.P. Dias Filho, The performance of a three-phase fluidized bed reactor in treatment of wastewater with high organic load, *Braz. J. Chem. Eng.* 21 (2) (2004) 219–227.
- [3] F.V.F. Araujo, L. Yokoyama, L.A.C. Teixeira, Remoção de cor em soluções de corantes reativos por oxidação com H<sub>2</sub>O<sub>2</sub>/UV, *Quim. Nova* 29 (1) (2006) 11–14.
- [4] J.-M. Herrmann, Heterogeneous photocatalysis: fundamentals and applications to the removal of various types of aqueous pollutants, *Catal. Today* 53 (1) (1999) 115–129.
- [5] H.L. Liu, Y.R. Chiou, Optimal decolorization efficiency of Reactive Red 239 by UV/TiO<sub>2</sub> photocatalytic process coupled with response surface methodology, *Chem. Eng. J.* 112 (1–3) (2005) 173–179.
- [6] M. Muruganandham, M. Swaminathan, Photocatalytic decolourisation and degradation of Reactive Orange 4 by TiO<sub>2</sub>-UV process, *Dyes Pigm.* 63 (2/3) (2006) 133–142.
- [7] M.S.T. Gonçalves, A.M.F.O. Campos, E.M.M.S. Pinto, P.M.S. Plasencia, M.J.R.P. Queiroz, Photochemical treatment of solutions of azo dyes containing TiO<sub>2</sub>, *Chemosphere* 39 (5) (1999) 781–786.
- [8] Y. Wang, Solar photocatalytic degradation of eight commercial dyes in TiO<sub>2</sub> suspension, *Water Res.* 34 (3) (2000) 990–994.
- [9] I. Koyuncu, Influence of dyes, salts and auxiliary chemicals on the nanofiltration of reactive dye baths: experimental observations and model verification, *Desalination* 154 (3) (2003) 79–88.
- [10] M. Muruganandham, N. Sobana, M. Swaminathan, Solar assisted photocatalytic and photochemical degradation of Reactive Black 5, *J. Hazard. Mater.* 137 (3) (2006) 1371–1376.
- [11] C. Lizama, J. Freer, J. Baeza, H.D. Mansilla, Optimized photodegradation of Reactive Blue 19 on TiO<sub>2</sub> and ZnO suspensions, *Catal. Today* 76 (2–4) (2002) 235–246.
- [12] C.A.K. Gouvêa, F. Wypych, S.G. Moraes, N. Durán, N. Nagata, P. Peralta-Zamora, Semiconductor-assisted photocatalytic degradation of reactive dyes in aqueous solution, *Chemosphere* 40 (4) (2000) 433–440.
- [13] N.M. Mahmoodi, M. Arami, N.Y. Limaee, N.S. Tabrizi, Kinetics of heterogeneous photocatalytic degradation of reactive dyes in an immobilized TiO<sub>2</sub> photocatalytic reactor, *J. Colloid Interface Sci.* 295 (1) (2006) 159–164.
- [14] P. Pekakis, N.P. Xekoukoulotakis, D. Mantzavinos, Treatment of textile dyehouse wastewater by TiO<sub>2</sub> photocatalysis, *Water Res.* 40 (6) (2006) 1276–1286.
- [15] L.B. Reutergeradh, M. langphasuk, Photocatalytic decolourization of reactive azo dye: a comparison between TiO<sub>2</sub> and CdS photocatalysis, *Chemosphere* 35 (3) (1997) 585–596.
- [16] T. Panswad, W. Luangdilok, Decolorization of reactive dyes with different molecular structures under different environmental conditions, *Water Res.* 34 (17) (2000) 4177–4184.
- [17] K. Vinodgopal, D.E. Wynkoop, P.V. Kamat, Environmental photochemistry on semiconductor surfaces: photosensitized degradation of a textile azo dye, *Acid Orange 7*, on TiO<sub>2</sub> particles using visible light, *Environ. Sci. Technol.* 30 (5) (1996) 1660–1666.
- [18] H. Lachheb, E. Puzenat, A. Houas, M. Ksibi, E. Elaloui, C. Guillard, J.-M. Herrmann, Photocatalytic degradation of various types of dyes (Alizarin S, Crocein Orange G, Methyl Red, Congo Red Methylene Blue), *Appl. Catal. B: Environ.* 39 (1) (2002) 75–90.
- [19] K. Tanaka, K. Padermpole, T. Hisanaga, Photocatalytic degradation of commercial azo dyes, *Water Res.* 34 (1) (2000) 327–333.
- [20] V.V. Tarasov, G.S. Barancova, N.K. Zaitsev, Z. Dongxiang, Photochemical kinetics of organic dye oxidation in water, *Process Saf. Environ. Prot.* 81 (B4) (2003) 243–249.
- [21] A.J. Julson, D.F. Ollis, Kinetics of dye decolorization in an air–solid system, *Appl. Catal. B: Environ.* 65 (3–4) (2006) 315–325.
- [22] A.V. Rupa, D. Manikandan, D. Divakar, T. Sivakumar, Effect of deposition of Ag on TiO<sub>2</sub> nanoparticles on the photodegradation of Yellow 17, *J. Hazard. Mater.* 147 (3) (2007) 906–913.
- [23] B. Neppolian, S.R. Kanel, H.C. Choi, M.V. Shankar, B. Arabindoo, V. Murugesan, Photocatalytic degradation of Reactive Yellow 17 dye in aqueous solution in the presence of TiO<sub>2</sub> with cement binder, *Int. J. Photoenergy* 5 (2) (2003) 45–49.
- [24] B. Neppolian, H.C. Choi, S. Sakthivel, B. Arabindoo, V. Murugesan, Solar/UV-induced photocatalytic degradation of three commercial textile dyes, *J. Hazard. Mater.* 89 (2–3) (2002) 303–317.
- [25] M. Janus, A.W. Morawski, New method of improving photocatalytic activity of commercial Degussa P25 for azo dyes decomposition, *Appl. Catal. B: Environ.* 75 (1–2) (2007) 118–123.